Molecular Therapy
Methods & Clinical Development
Original Article

Germline CRISPR/Cas9-Mediated Gene Editing Prevents Vision Loss in a Novel Mouse Model of Aniridia

Seyedeh Zeinab Mirjalili Mohanna,[1,2] Jack W. Hickmott,[1,2] Siu Ling Lam,[1] Nina Y. Chiu,[1,2] Tess C. Lengyell,[1] Beatrice M. Tam,[3] Orson L. Moritz,[3] and Elizabeth M. Simpson[1,2]

[1]Centre for Molecular Medicine and Therapeutics at British Columbia Children's Hospital, The University of British Columbia, Vancouver, BC V5Z 4H4, Canada; [2]Department of Medical Genetics, The University of British Columbia, Vancouver, BC, Canada; [3]Department of Ophthalmology and Visual Sciences and Centre for Macular Research, The University of British Columbia, Vancouver, BC, Canada

Aniridia is a rare eye disorder, which is caused by mutations in the paired box 6 (*PAX6*) gene and results in vision loss due to the lack of a long-term vision-saving therapy. One potential approach to treating aniridia is targeted CRISPR-based genome editing. To enable the *Pax6* small eye (*Sey*) mouse model of aniridia, which carries the same mutation found in patients, for preclinical testing of CRISPR-based therapeutic approaches, we endogenously tagged the *Sey* allele, allowing for the differential detection of protein from each allele. We optimized a correction strategy *in vitro* then tested it *in vivo* in the germline of our new mouse to validate the causality of the *Sey* mutation. The genomic manipulations were analyzed by PCR, as well as by Sanger and next-generation sequencing. The mice were studied by slit lamp imaging, immunohistochemistry, and western blot analyses. We successfully achieved both *in vitro* and *in vivo* germline correction of the *Sey* mutation, with the former resulting in an average 34.8% ± 4.6% SD correction, and the latter in restoration of 3xFLAG-tagged PAX6 expression and normal eyes. Hence, in this study we have created a novel mouse model for aniridia, demonstrated that germline correction of the *Sey* mutation alone rescues the mutant phenotype, and developed an allele-distinguishing CRISPR-based strategy for aniridia.

INTRODUCTION

The paired box 6 (*PAX6*) gene encodes a transcription factor that controls many aspects of early development of the central nervous system, eye, and some non-neuronal tissues such as the pituitary and pancreas.[1] This transcription factor is conserved in evolution and has complex regulatory regions that span beyond 200 kb.[2] Heterozygous loss-of-function mutations of *PAX6* result in a rare congenital eye disorder known as aniridia.[3] Patients with aniridia are typically born with low vision, mainly due to fovea hypoplasia, and become legally blind in young adulthood due to progressive sight-threatening complications, including glaucoma, cataract, and corneal opacification.[4] Currently, there are no long-term vision-saving therapies or cures for aniridia; however, some of the secondary ocular abnormalities can be partially managed through medical and surgical interventions with limited success, as surgeries on aniridic eyes can expedite aniridia-related keratopathy and worsen vision.[5,6] Therefore, new treatment strategies are needed for aniridia.

One possible approach to treating aniridia is gene therapy, where genetic material is delivered into cells to make the required protein (augmentation) or correct the defective gene (gene editing).[7] However, similar to haploinsufficiency, *PAX6* overexpression has been shown to negatively affect normal eye development.[8–11] Thus, very precise regulation of *PAX6* would be necessary to achieve therapeutic success with augmentation gene therapy.[12] In contrast, gene editing, for example by clustered regularly interspaced short palindromic repeats (CRISPR), can be used to revert a mutation to the correct sequence in the genome,[13] thereby allowing for the normal regulation of expression levels and timing in appropriate cell types. Unfortunately, CRISPR-mediated gene editing can also create small insertions and deletions (indels), or even large deletions and complex rearrangements, which are important considerations when taking this approach.[14]

Studies on cellular and animal models are often the first steps toward developing a gene therapy. In the case of aniridia, this approach is supported by the fact that the human *PAX6* gene is homologous to the mouse *Pax6* gene, and the protein products from these two genes have identical amino acid sequences.[15] The small eye (*Sey*) mouse was first described in 1996 and is a widely accepted model for aniridia, which carries a spontaneous point mutation causing a premature stop codon in exon 8 of the *Pax6* gene.[16–18] Mice that are homozygous for the *Sey* allele are anophthalmic and die shortly after birth, whereas mice that are heterozygous for *Sey* are viable and exhibit iris hypoplasia, lens abnormalities, and corneal clouding.[17–19] In both cases, the

Received 19 February 2020; accepted 9 March 2020;
https://doi.org/10.1016/j.omtm.2020.03.002.

Correspondence: Elizabeth M. Simpson, Centre for Molecular Medicine and Therapeutics at British Columbia Children's Hospital, The University of British Columbia, 3020-950 West 28th Avenue, Vancouver, BC V5Z 4H4, Canada.
E-mail: simpson@cmmt.ubc.ca

 © 2020 The Author(s).
This is an open access article under the CC BY-NC-ND license (http://creativecommons.org/licenses/by-nc-nd/4.0/).

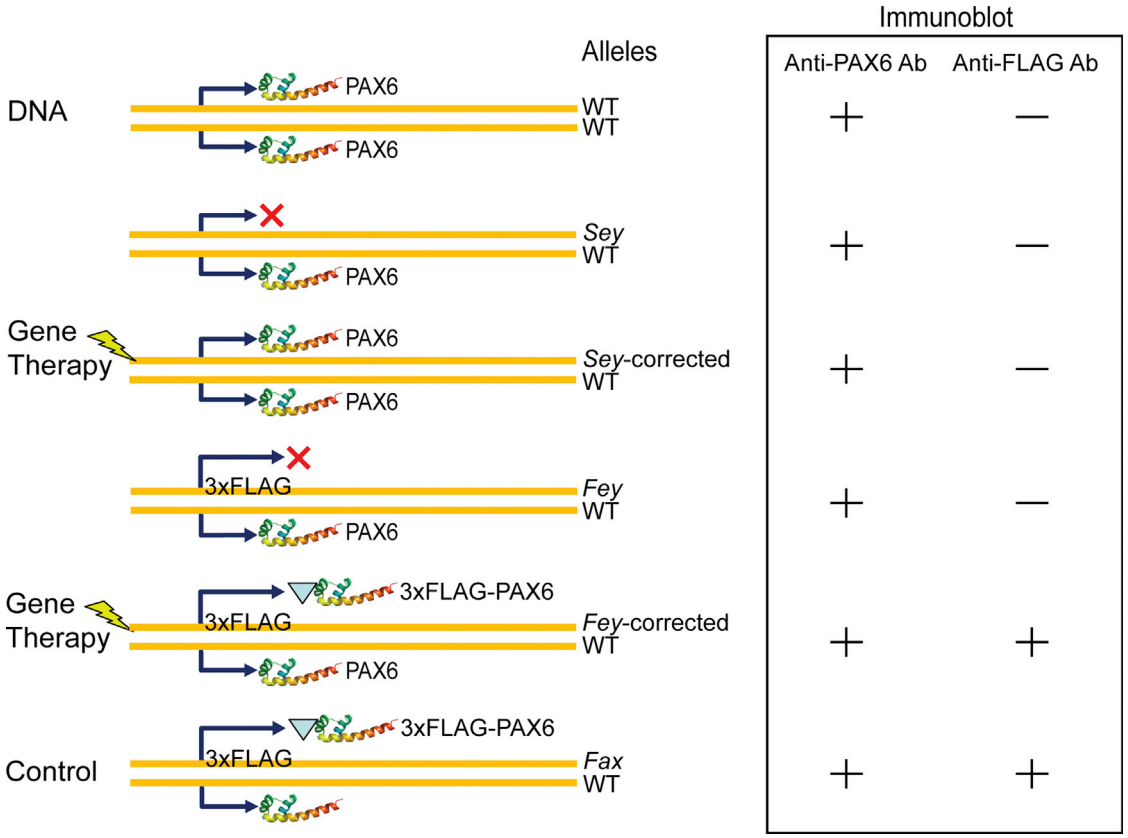

Figure 1. Generation of a New Transgenic Mouse Model of Aniridia for Quantifying the Impact of CRISPR Therapy

Sey mice are not optimal for testing CRISPR-based therapeutic approaches for aniridia, as the CRISPR-corrected protein would not differ from the wild-type (WT) counterpart. Insertion of a 3xFLAG tag on the *Sey* allele will enable quantitative assessment of our *Pax6* gene editing therapy by creating a corrected form that can be distinguished from WT by antibody labeling. Inserting the same tag on the WT allele will create an essential control mouse to ensure that the addition of the 3xFLAG tag does not interfere with the PAX6 protein function. Ab, antibody; *Fax*, FLAG-tagged *Pax6*; *Fey*, FLAG-tagged *Sey*; *Sey*, *Pax6* small eye.

phenotypes are comparable in humans, with the latter modeling aniridia.[19,20] Furthermore, the mutation present in *Sey* mice (G194X) has been reported in a patient with aniridia,[21] making *Sey* an exciting model for proof-of-principle gene therapy studies.

Given the role of PAX6 in stem/progenitor cells,[22] and the overall plasticity of the eye,[23,24] we think a postnatal CRISPR-based gene therapy is a feasible option for treating aniridia. Supporting this is evidence of successful delivery of CRISPR/CRISPR-associated protein 9 (Cas9) components via viral vectors to rodent and non-human primate eyes,[25–30] as well as the ability of the aniridic mouse eye to improve after augmenting PAX6 levels postnatally.[23,24] Therefore, we hypothesized that increasing the expression of PAX6 through a CRISPR-based gene-editing strategy would improve the structure and function of the eye, and ultimately rescue the mutant phenotype in a mouse model of aniridia.

For *in vivo* CRISPR strategy development, it would be advantageous to have a mouse model that allows us to distinguish both the gene and protein of wild-type (WT) PAX6 from CRISPR-corrected mutant PAX6, for quantification of the targeted genome editing efficacy (Figure 1). Thus, using CRISPR for endogenous-gene tagging, we have created a new model for preclinical CRISPR-based therapy development for aniridia. Furthermore, since the *Sey* mutation was first identified more than half a century ago, there was a possibility that the *Sey* locus might have acquired additional genetic mutations over time.[16] Hence, as an important step, we validated the causality of this mutation by germline correction. Lastly, we developed a CRISPR allele-distinguishing strategy that successfully corrected the *Sey* mutation both *in vitro* and *in vivo* in the mouse germline.

RESULTS

PAX6 and 3xFLAG/*PAX6* Constructs Induced Ectopic Eyes in *Xenopus laevis* Tadpoles

Sey mice produce WT PAX6 protein, so to distinguish the CRISPR-corrected PAX6 protein from WT, a protein tag was necessary. To tag PAX6, FLAG tag was selected, as it is small,[31] can be stained with high-affinity monoclonal antibodies,[32] and has been previously used for endogenous *Pax6* tagging *in vivo*.[33] Triple FLAG (3xFLAG) tag was selected over single FLAG tag, as it is easier to detect with

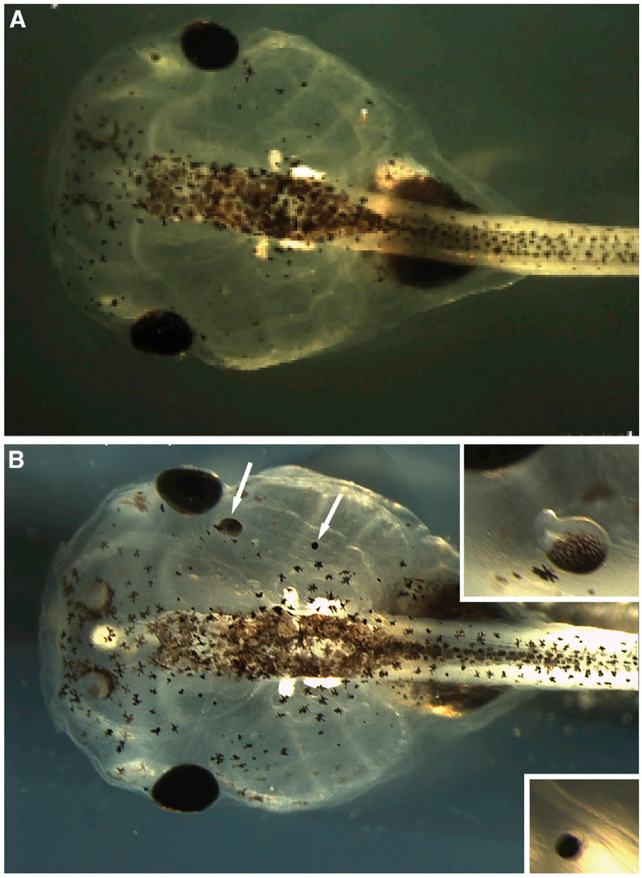

C

Construct	Tadpoles	Ectopic Eyes	Ectopic RPE
Water	208	0 (0.00%)	0 (0.00%)
EmGFP	412	0 (0.00%)	1 (0.24%)
PAX6	251	5 (1.99%)	18 (7.17%)
3xFLAG/*PAX6*	329	9 (2.74%)	6 (1.82%)
PAX6/3xFLAG	349	1 (0.29%)	1 (0.29%)

Figure 2. FLAG Tag Does Not Disrupt the Ability of PAX6 to Induce Ectopic Eyes in *Xenopus laevis*

X. laevis embryos were injected with mRNA encoding one of: emerald GFP (EmGFP), PAX6, N-terminally or C-terminally 3xFLAG-tagged PAX6 (3xFLAG/PAX6 and PAX6/3xFLAG, respectively), and scored 14 days later for the development of ectopic eyes and retinal pigment epithelium (RPE). (A) Example of a non-injected *X. laevis* tadpole, with one eye on each side of the head. (B) Example of a *PAX6* mRNA-injected *X. laevis* tadpole, with two additional ectopic eyes (arrows). Insets are magnifications of each ectopic eye. (C) Quantification of ectopic eye formation in *X. laevis* tadpoles.

antibodies.[32,34] PAX6 is highly conserved between diverse species,[35] and it is a concern that endogenous gene tagging may cause a functional deficit. However, evidence showing successful use of N-terminally tagged PAX6 in *in vitro* experiments[36–38] supported the possibility of tagging this protein. Overexpression of *Pax6* induces the formation of ectopic eyes in *Xenopus laevis* (*X. laevis*).[33] Therefore, to determine whether the 3xFLAG-tagged PAX6 remains functional, N- and C-terminally tagged human *PAX6* cDNA constructs were tested in a rapid ectopic eye formation assay. *X. laevis* embryos were injected with mRNA encoding emerald GFP (EmGFP), PAX6, N-terminally 3xFLAG-tagged PAX6 (3xFLAG/PAX6), or C-terminally 3xFLAG-tagged PAX6 (PAX6/3xFLAG). The resulting tadpoles were examined 14 days later for the formation of ectopic eye structures (Figure 2). *PAX6*, 3xFLAG/*PAX6*, and *PAX6*/3xFLAG constructs, but not EmGFP or water, induced ectopic eyes, confirming the functionality of all three constructs. The N-terminally tagged PAX6 was selected for future use, as it produced the greatest number of ectopic eyes.

An Optimized CRISPR Strategy Successfully Inserted 3xFLAG Tag in Mouse Embryonic Stem Cells

Guide RNA (gRNA) and single-stranded oligodeoxynucleotide (ssODN) template designs can tip the balance toward more successful gene editing, and therefore optimizing CRISPR/Cas9 system components prior to *in vivo* studies is an important step. The N-terminal 3xFLAG-tag location was based on our results with the ectopic eye formation assay in *X. laevis* tadpoles. To improve the gene editing efficiency, and to readily use the optimized CRISPR strategy in the microinjection, we used the Cas9 ribonucleoprotein (RNP) complex. The Cas9 RNP complexes with their corresponding ssODNs were electroporated into mouse embryonic stem cells (ESCs), and the outcome of genomic manipulation was quantified by site-specific next-generation sequencing (NGS). Figure 3A shows the schematic of our best CRISPR strategy for addition of the 3xFLAG tag at the *Pax6* start codon (ATG) that was able to successfully insert the intact 3xFLAG tag in 1,007 out of 19,573 NGS reads (5.14%) (Figure 3B). In 7,986 out of 19,573 reads (40.8%), Cas9-induced double-stranded breaks were repaired by the non-homologous end joining (NHEJ) pathway, creating relatively small indels in close vicinity to the cut site.

Endogenous *Sey* Tagging Created a Novel Mouse Model for Aniridia without Compromising the Protein Function in the Control Mice

We used an earlier *in vitro*-optimized CRISPR strategy (Figure 3A) to insert a 3xFLAG tag to the *Sey* allele in mouse zygotes in a rapid manner, creating the 3xFLAG-tagged *Sey* mouse strain (C57BL/6J [B6]-*Pax6*$^{Sey\text{-}em1(3xFLAG)Ems}$), called *Fey* hereafter. Since the *Sey* mutation causes a premature stop codon and no detectable protein,[39] we were unable to directly characterize the function of the *Fey* allele. Thus, we created the matched WT control strain (B6-*Pax6*$^{em3(3xFLAG)Ems}$), called *Fax* hereafter. Both strains were backcrossed to WT B6 mice to remove any incidental mutations. As expected, the slit lamp imaging of adult *Fey* mouse eyes revealed abnormalities comparable to those seen in *Sey* mice. However, even when required for the entire eye development in a complex and sophisticated mammalian system, the addition of the 3xFLAG tag to the conserved PAX6 in *Fax* mice resulted in no eye phenotypes (Figure 4A). Moreover, we scored eye size and corneal cloudiness by visual inspection in 106 homozygous *Fax* and 76 WT eyes. We found no significant difference in the ocular phenotype between

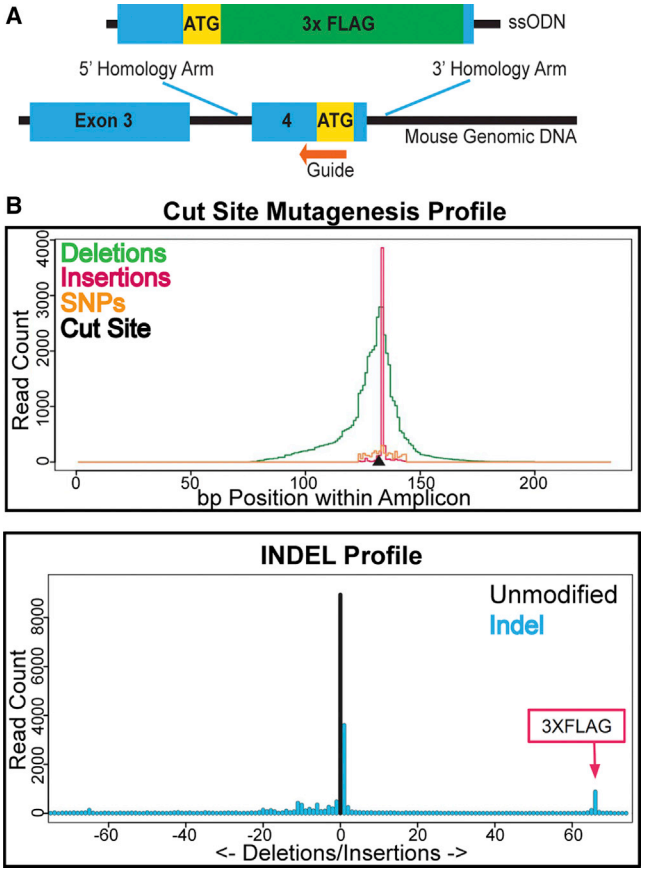

Figure 3. Site-Specific Next-Generation Sequencing Revealed the Correct Insertion of 3xFLAG Tag in 5.14% of Sequences

Cas9 ribonucleoprotein complexes were assembled *in vitro* and electroporated into mouse embryonic stem cells. Site-specific next-generation sequencing was used to quantify the knock-in. (A) Schematic of the best guide RNA (gRNA) and single-stranded oligodeoxynucleotide (ssODN) for CRISPR/Cas9-mediated insertion of a 3xFLAG tag at *Pax6* ATG (yellow). In addition to the tag sequence (green), the ssODN contained 60-bp homology arms flanking the Cas9-induced double-stranded break. Blue indicates *Pax6* exons; black indicates *Pax6* introns. The diagram is not to scale. (B) The top panel shows mutation positions relative to the Cas9 cut site. 1,007 out of 19,573 reads (5.14%) showed the correct 3xFLAG insertion. The bottom panel shows the insertion and deletion (indel) size distribution.

homozygous *Fax* and WT mice (one-tailed t test, p = 0.490). Left eyes from a subset of these mice (eight WT and eight homozygous *Fax* mice) were examined by slit lamp, predominantly for possible abnormalities in the lens, which could not be assessed by visual inspection (Figure S1). We found no significant difference in the lens structure between homozygous *Fax* and WT mouse eyes (one-tailed t test, p = 0.074). Immunohistological analysis was performed to look at the co-localization and expression of PAX6 and 3xFLAG-tagged PAX6 proteins. Sections from *Sey*, *Fey*, WT, and *Fax* retinas showed similar anti-PAX6 staining patterns in the ganglion cell layer (GCL) and inner nuclear layer (INL). Additionally, for *Fax* retinas, co-labeling of PAX6 and FLAG was detected in both the GCL and INL (Figure 4B).

Sey Mutation Was Efficiently Corrected in Mouse ESCs

Optimization of CRISPR/Cas9 components in cells enabled us to ensure on-target cleavage activity and specificity prior to *in vivo* studies. One recent approach that has been quite successful in distinguishing alleles uses Cas proteins with unique protospacer adjacent motifs (PAMs) such that correcting the mutation removes the PAM.[40–42] However, this approach is restricted by the PAM sequences available, and it is currently not applicable to the *Sey* mutation. We worked with mouse $Pax6^{Sey/Sey}$ and $Pax6^{+/+}$ ESCs, as homozygosity made it easier to interpret modifications from sequencing chromatograms. The on-target cleavage activity was determined by Sanger sequencing of edited whole-cell lysates normalized against unedited controls (defined as either $Pax6^{Sey/Sey}$ or $Pax6^{+/+}$ ESCs electroporated with Cas9 and an ssODN template in the absence of gRNA). According to the results, our best CRISPR strategy corrected the *Sey* mutation with a 42.9% success rate and modified the PAM with a rate of 41.4% to avoid repeated targeting of edited alleles (Figure 5A). Upon repeating the *in vitro* gene editing in triplicate, the average correction rate for the *Sey* mutation was 34.8% ± 4.6% (mean ± standard deviation), while the average PAM change rate was 42.9% ± 3.2%. In a head-to-head experiment, our best CRISPR strategy was then tested in both $Pax6^{Sey/Sey}$ and $Pax6^{+/+}$ ESCs to determine its specificity. Quantification of the PAM change in these cells revealed a 2-fold enrichment of gRNA interaction with the mutant allele.

CRISPR/Cas9-mediated gene editing is known to lead to sequence heterogeneity among cells from the same sample.[43] Hence, to look at the samples at a single molecule level, we sent $Pax6^{Sey/Sey}$ and $Pax6^{+/+}$ whole-cell lysates edited with our best CRISPR strategy and the unedited controls for site-specific NGS, which enabled us to observe the various on-target mutations that CRISPR created. As expected, in the unedited $Pax6^{Sey/Sey}$ sample, most of the NGS reads (11,404/11,458; 99.5%) aligned completely to the reference sequence. The remainder of the reads in the unedited sample had single nucleotide substitutions, which could be explained by the error rate associated with this sequencing technique.[44] Among the 18,291 aligned reads for the edited $Pax6^{Sey/Sey}$ sample, 3,644 reads (19.9%) had both knock-in variants with no further changes in *Pax6* exon 8; 5,162 reads (28.2%) had both knock-in variants and no undesired changes within a 20-bp window; 6,608 reads (36.1%) showed the correction of *Sey* mutation; 6,893 reads (37.7%) had the PAM change; and, lastly, 7,855 reads (42.9%) remained unmodified (i.e., still had the *Sey* mutation). The indel profile analysis revealed various sizes of NHEJ-induced indels around the Cas9 cut site (Figure 5B). Consistent with the earlier Sanger sequencing results, the indel frequency analysis of edited $Pax6^{Sey/Sey}$ and $Pax6^{+/+}$ samples showed a 2-fold enrichment of gRNA interaction with the mutant allele.

In Vivo Gene Editing Corrected the *Sey* Mutation with a 25% Success Rate

Rescuing the mutant phenotype by correcting the *Sey* mutation in the mouse germline proves causality and serves as a proof-of-principle experiment for a future somatic gene therapy. The corrected mice were generated by microinjecting the *in vitro*-optimized CRISPR

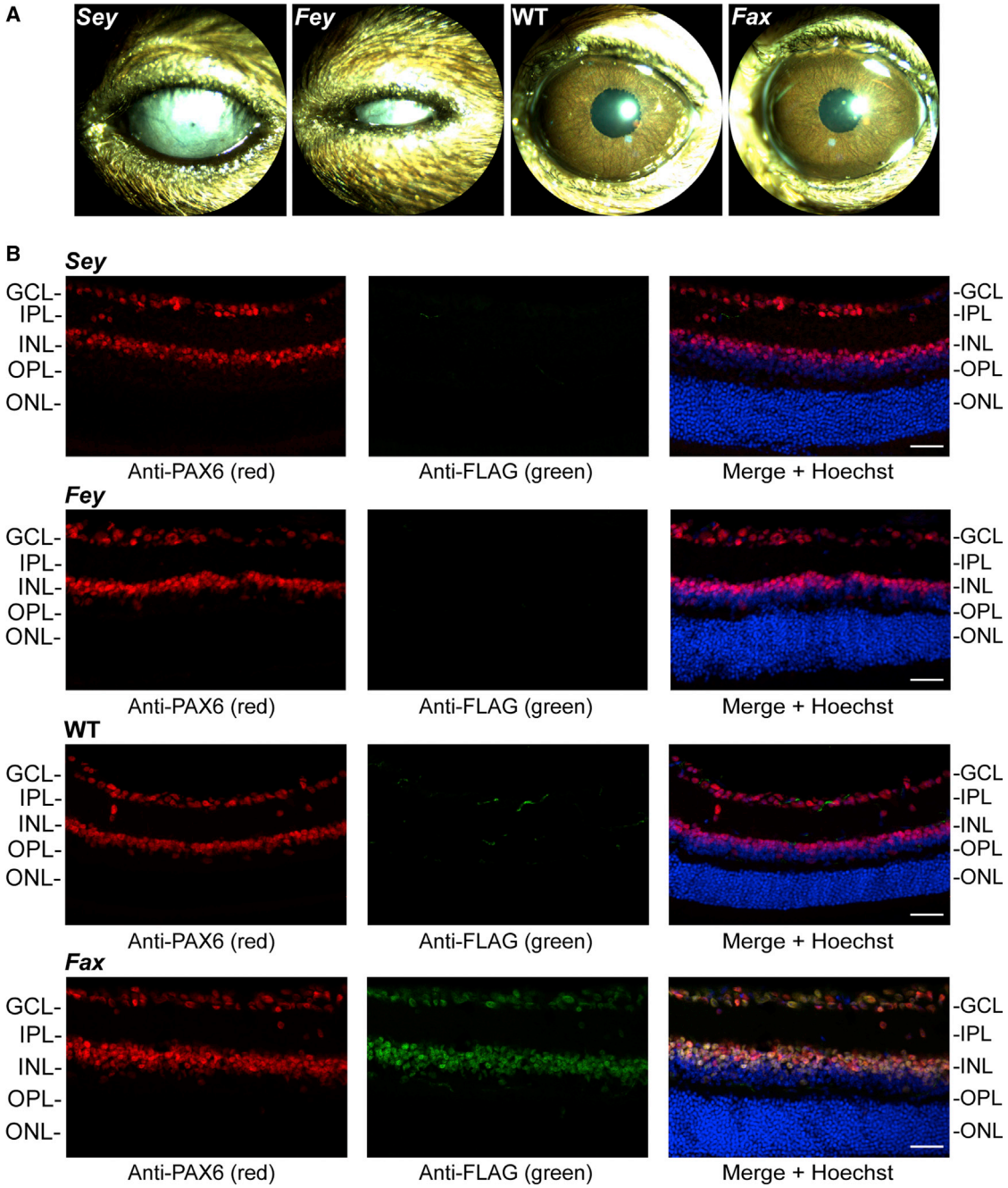

Figure 4. *Fey* Is a Novel Mouse Model of Aniridia and, Importantly, the *Fax* Control Mice Showed No Phenotype

An optimized Cas9 ribonucleoprotein complex and a single-stranded oligodeoxynucleotide containing the 3xFLAG sequence were microinjected into one-cell mouse zygotes to generate transgenic animals in one step. (A) Slit lamp analysis of the transgenic mouse eyes. As expected, images of *Fey* showed small eyes and corneal opacity, not significantly different from the *Sey* (*Pax6* small eye) mouse model (two-tailed test, $p > 0.999$). Slit lamp images of *Fax* (FLAG-tagged *Pax6*) mouse eyes showed normal iris and clear cornea, which were not significantly different from WT eyes (one-tailed t test, $p > 0.999$). *Fax*, FLAG-tagged *Pax6*; *Fey*, FLAG tagged *Sey*; *Sey*, *Pax6* small eye; WT, wild-type. (B) Histological analysis of mouse retinas. Adult mouse eyes were directly fixed and stained with FLAG and PAX6 antibodies. While FLAG staining was absent in the negative controls (*Fey* and WT retinas), *Fax* mouse retinas showed positive co-labeling of FLAG and PAX6. GCL, ganglion cell layer; IPL, inner plexiform layer; INL, inner nuclear layer; OPL, outer plexiform layer; ONL, outer nuclear layer. Blue shows Hoechst staining. All images were taken at the same magnification. Scale bars, 34 μm.

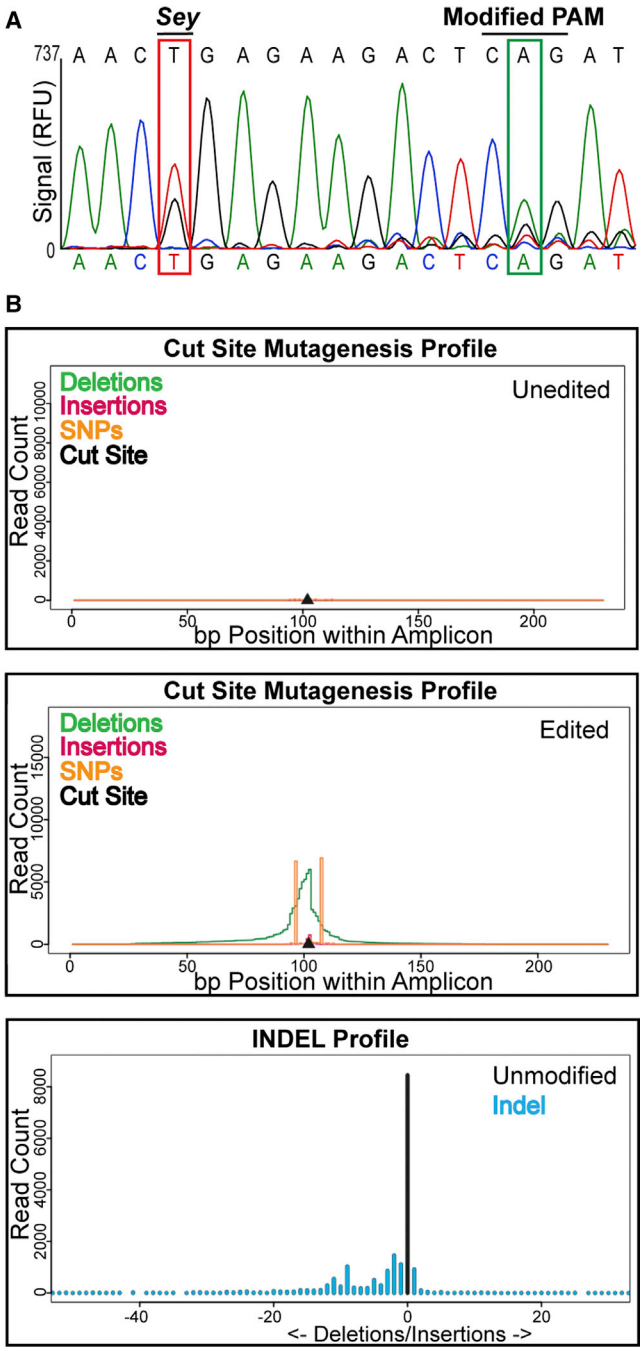

Figure 5. *In Vitro* CRISPR-Mediated Gene Editing Corrects the *Sey* Mutation in *Pax6*$^{Sey/Sey}$ Embryonic Stem Cells

Sey is a point mutation where the wild-type G nucleotide is mutated to a T, resulting in a premature stop codon. Various CRISPR-mediated editing strategies to correct the *Sey* mutation were tested in mouse embryonic stem cells, and the editing efficiencies were quantified by Sanger sequencing and site-specific next-generation sequencing (NGS). (A) Sanger sequencing chromatogram of the best CRISPR strategy. Sanger sequencing revealed a correction rate from T to G of 42.9% (red box). To prevent repeat targeting of previously edited alleles, the single-stranded oligodeoxynucleotide (ssODN) also included a silent base change in the protospacer adjacent motif (PAM) sequence, giving an alteration rate from G to A of 41.4% (green box). RFU, relative fluorescent units. (B) Site-specific NGS histograms of the best CRISPR strategy. 11,404 out of 11,458 (99.5%) reads from the unedited cells (negative control) matched the reference sequence. For the cells edited with the best strategy, 3,644 out of 18,291 reads (19.9%) had both the correction and the PAM change with no other changes in *Pax6* exon 8. 7,855 out of 18,291 reads (42.9%) were unmodified.

gene editing strategy into *Pax6*$^{Fey/+}$ and *Pax6*$^{+/+}$ zygotes. Fifteen potential founder mice were born. A summary of the phenotyping, genotyping, and sequencing results of these mice is presented in Table 1. The proportion of animals with eye abnormalities observed by visual inspection was 46.7% (7/15), which was not significantly different from the expected 50:50 phenotypic ratio of *Sey* to WT. Moreover, the FLAG allele was present at 26.7% (8/30), which again was not significantly different from the expected 25%. Mice 1-9 and 1-12 were positive for 3xFLAG, which was genetically linked to the *Sey* allele, but had a normal eye phenotype. Sequencing results of ear notches from these two mice confirmed the correction of *Sey* mutation and presence of the silent base change at the original PAM site. On the allelic level, we achieved a correction rate of 25% (2/8) for the *Fey* allele. Sequencing results also revealed that the WT allele was hit at a rate of 22.7% (5/22), while only 13.6% (3/22) of this rate represents a deleterious hit. All 8 FLAG alleles were hit by our CRISPR strategy, whereas 77.3% (17/22) of WT alleles remained unmodified.

Germline Correction of the *Sey* Mutation Restored 3xFLAG-Tagged PAX6 Expression and Normal Eyes

Upon breeding, founders 1-9 and 1-12 were shown to stably transmit the transgene to their progeny. A first pedigree mouse was chosen for each founder, resulting in establishment of two new transgenic strains, B6-*Pax6*$^{Fey\text{-}em4(c.[580TG;591GA])Ems}$ and B6-*Pax6*$^{Fey\text{-}em5(c.[580TG;591GA])Ems}$, which are called hereafter *Fey* correction *em4* (*FeyCor*^{em4}) and *Fey* correction *em5* (*FeyCor*^{em5}), respectively. Both strains were backcrossed to WT B6 mice to remove any incidental mutations. Excitingly, unlike *Fey* mice, *FeyCor*^{em4} and *FeyCor*^{em5} mouse eyes were not significantly different from WT by slit lamp examination (one-tailed t test, $p > 0.999$) (Figure 6A). Additionally, FLAG and PAX6 co-labeling in the immunohistological analysis of mouse retinas from both *FeyCor* strains confirmed the expression of 3xFLAG-tagged PAX6 in the GCL and INL (Figure 6B).

PAX6 Level Was Increased in the Brain of Germline-Corrected Mice

Being homozygous for a *Pax6* or *PAX6* null mutation causes anophthalmia and is neonatal lethal in both mice and humans, respectively.[17,45] Therefore, to examine PAX6 levels in an expressing tissue, we decided to perform western blot analysis on brain samples isolated from fetuses at embryonic day 18.5 (E18.5). PAX6 level influenced the phenotype of fetuses as expected, with *Pax6*$^{Fey/+}$ *and Pax6*$^{Fey/Fey}$ fetuses showing microphthalmia and anophthalmia, respectively, while *Pax6*$^{Fax/+}$ and *Pax6*$^{Fax/Fax}$ control fetuses had normal eyes. The germline correction of *Sey* mutation led to *Pax6*$^{FeyCor/+}$ and *Pax6*$^{FeyCor/FeyCor}$ fetuses having normal eyes that were not

Table 1. The *Sey* Phenotype Was Rescued In Two Mice By Germline Correction

Mouse ID	Eye Phenotype	3xFLAG Genotype	*Fey* Allele Corrected and PAM Change	*Fey* Allele Indel	Fey Allele Unedited	WT Allele Change[a]	WT Allele Indel	WT Allele Unedited
1-1	abnormal	F/+	NA	✓	NA	NA	NA	✓
1-2	abnormal	F/+	NA	✓	NA	NA	NA	✓
1-3	normal	+/+	NA	NA	NA	NA	✓	✓
1-4	normal	+/+	NA	NA	NA	NA	✓	✓
1-5	abnormal	F/+	NA	✓	NA	NA	NA	✓
1-6	abnormal	F/+	NA	✓	NA	NA	NA	✓
1-7	abnormal	F/+	NA	✓	NA	NA	NA	✓
1-8	normal	+/+	NA	NA	NA	NA	NA	✓✓
1-9	normal	F/+	✓	NA	NA	NA	NA	✓
1-10	normal	+/+	NA	NA	NA	✓	NA	✓
1-11	normal	+/+	NA	NA	NA	NA	NA	✓✓
1-12	normal	F/+	✓	NA	NA	✓	NA	NA
1-13	abnormal	+/+	NA	NA	NA	NA	✓	✓
1-14	abnormal	F/+	NA	✓	NA	NA	NA	✓
1-15	normal	+/+	NA	NA	NA	NA	NA	✓✓
	7/15 (46.7%)[b]	8/30 (26.7%)[c]	2/8 (25.0%)[d]	6/8 (75.0%)[d]	0/8 (0%)[d]	2/22 (9.10%)[e]	3/22 (13.6%)[e]	17/22 (77.3%)[e]

F, 3xFLAG-tagged *Pax6* allele; +, wild-type *Pax6* allele; ID, identifier; Indel, insertion or deletion; WT, wild-type *Pax6*; ✓, present in one allele; ✓✓, present in both alleles; NA, not applicable.
[a]This refers to either a PAM change or point mutations with no effect on the phenotype.
[b]Abnormal/total ratio.
[c]Allele of interest/total alleles.
[d]Allele of interest/total *Fey* alleles.
[e]Allele of interest/total WT alleles.

significantly different from WT (one-tailed t test, $p > 0.999$) (Figure S2). Next, we looked at PAX6 levels using western blotting. Immunoblots of E18.5 brains showed co-staining of 3xFLAG-tagged PAX6 and PAX6 proteins for the *FeyCor* genotype, suggesting that the rescue of 3xFLAG-tagged PAX6 expression in the brain of these fetuses (Figure 7A). PAX6 protein levels were determined from two technical replicates with an understanding of the semiquantitative nature of these results. For each immunoblot, PAX6 protein levels were normalized against a non-specific protein revealed by the secondary antibody (Figure 7B). See Table S2 for relative PAX6 levels in each sample. Statistical analysis revealed a significant decrease in PAX6 levels in the brains of heterozygous *Fey* fetuses compared to homozygous *FeyCor* fetuses (one-tailed t test, $p = 0.017$), while no significant difference was observed in the mean PAX6 levels between homozygous *FeyCor* and WT genotypes (two-tailed t test, $p = 0.999$). As expected, statistical analysis also revealed similar PAX6 levels in the brains of homozygous *Fax* and WT fetuses (two-tailed t test, $p = 0.937$), which was significantly more than brains from heterozygous *Fey* fetuses (one-tailed t test, $p = 0.016$), confirming the observation that the *Pax6* genotype, but not the endogenous tagging, influences PAX6 protein levels.

DISCUSSION

Aniridia was first described in 1818.[46] Despite considerable research efforts during the past 200 years, there remains a therapeutic gap for aniridia patients around the world. Therapy development for rare diseases such as aniridia relies heavily on efficacy and safety studies performed on animal models. In this study, we developed a new mouse model of aniridia, *Fey*, with the addition of 3xFLAG to the *Sey* allele, that can be used to explore gene-editing therapies for this debilitating disease.

Prior to making *Fey*, we tested the impact of the 3xFLAG tag on WT *Pax6*, naming this allele *Fax*. We were surprised that the heterozygous, and even homozygous, addition of 3xFLAG to *Pax6 in vivo* did not result in any observed undesired phenotypes in the "control" *Fax* mice, suggesting that our endogenous gene tagging did not influence the function of PAX6. This is critical since it shows that when the *Fey* mouse is "corrected", the new allele will be fully functional. However, note that we focused our characterization on the ocular phenotype, since aniridia is primarily an eye-related disorder, and thus we cannot rule out the possibility of other subtle phenotypes in non-ocular *Pax6*-expressing tissues.

Sey is an old mutation,[16] and thus this non-functional allele could have undergone random genetic drift during the at least 52 years of continuous breeding since discovery. Such additional mutations could be difficult to detect even by sequencing if located in non-coding *Pax6* regulatory elements.[47] The success of our mutation-dependent

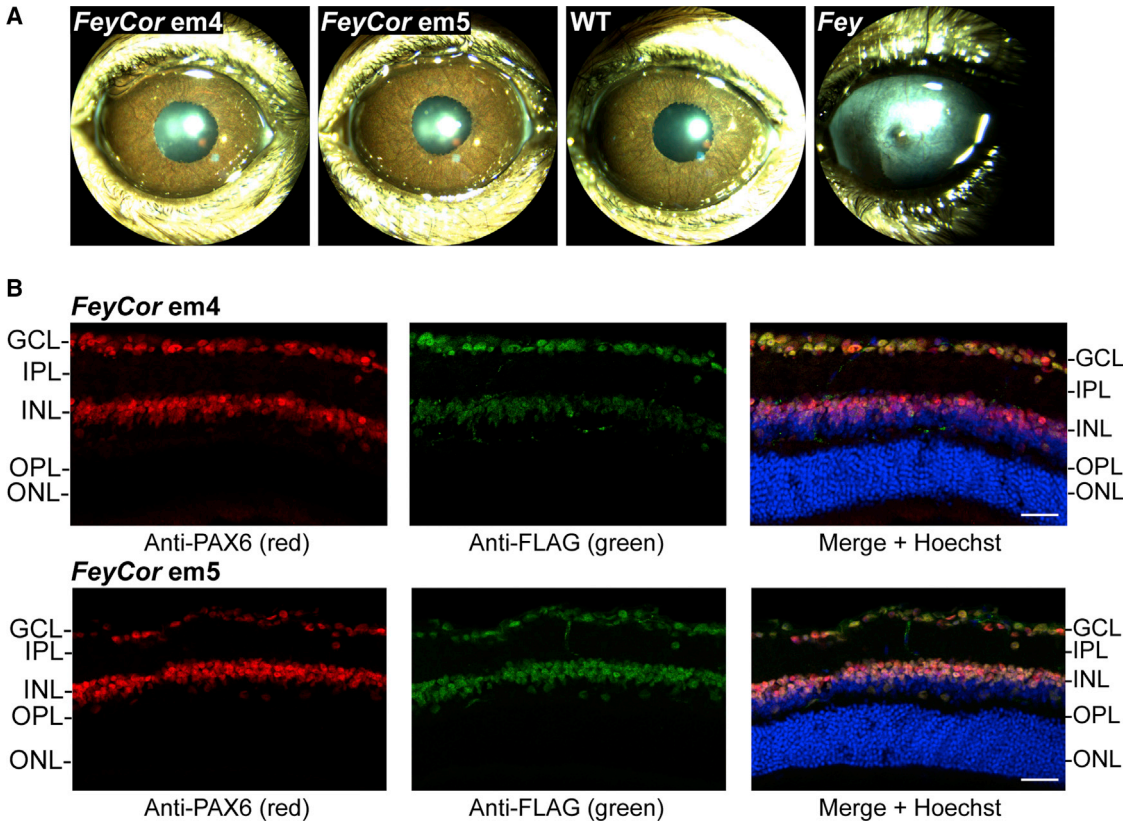

Figure 6. Germline Correction of the *Sey* Mutation Rescued the Mutant Eye Phenotype

To correct the *Sey* mutation *in vivo*, an optimized CRISPR-mediated editing strategy was microinjected into one-cell mouse zygotes. Progeny of founders with inheritable transmission of the transgene were subjected to phenotypical characterization and *Pax6* expression analysis. (A) Slit lamp images of *Fey* corrected (*FeyCor*) mouse eyes demonstrated clear cornea and normal iris comparable to WT mouse eyes, and distinctly none of the *Fey* eye abnormalities. *Fey*, FLAG-tagged *Sey*; *Sey*, *Pax6* small eye; WT, wild-type. (B) Positive co-labeling of FLAG and PAX6 was observed in the histological analysis of mouse retinas from both *FeyCor* strains. GCL, ganglion cell layer; IPL, inner plexiform layer; INL, inner nuclear layer; OPL, outer plexiform layer; ONL, outer nuclear layer. Blue shows Hoechst staining. All images were taken at the same magnification. Scale bars, 34 μm.

CRISPR strategy relied on the causality of the *Sey* mutation. Therefore, as an important step, we validated the causality of the *Sey* mutation in the *Fey* mouse through a CRISPR-based germline correction experiment and demonstrated that correction of just this 1 bp fully restored the ocular phenotype to WT. These results further validate *Fey* as a novel mouse model for the development of CRISPR-based mutation correcting therapies.

The *Fey* mouse will also be valuable for the development and quantification of efficacy for numerous other therapeutic approaches. For example, nonsense suppression therapies using readthrough compounds such as G418, amlexanox, and ataluren to overcome the presence of nonsense mutations in aniridia. G418 has shown readthrough activity both *in vitro* and *in vivo*,[48–50] and amlexanox has shown activity *in vitro*.[51,52] Ataluren has shown activity in mice,[24,53] and has been in clinical trial for aniridia (ClinicalTrials.gov: NCT02647359). *Fey* mice can be also used to design and explore CRISPR/Cas13 strategies that target *Pax6* mutations at the RNA level without permanently altering the genome.[54] Additionally, mutation-independent strategies such as the intronic insertion of the *Pax6* cDNA sequence immediately downstream of the AUG, as well as use of the spliceosome-mediated RNA *trans*-splicing (SMaRT) technique, will benefit from having the new protein FLAG tagged. The former and the latter therapeutic approaches have been shown to be effective in treating mouse models of hemophilia[55] and retinitis pigmentosa,[56] respectively.

We successfully achieved both *in vitro* and *in vivo* germline correction of the *Sey* and *Fey* mutations, respectively, restoring the mutant protein expression. *In vitro* delivery by electroporation into ESCs resulted in an average 34.8% ± 4.6% SD correction, while *in vivo* delivery by microinjection into zygotes resulted in 25% correction. Furthermore, the bias toward the mutant allele was 2-fold and 4-fold higher in our *in vitro* and *in vivo* experiments, respectively. Thus, although both were successful, our allele-distinguishing CRISPR strategy performed quite differently depending on the delivery method and recipient cell. Therefore, we now hypothesize that the effectiveness of this strategy when delivered by viral or non-viral delivery vectors to somatic cells

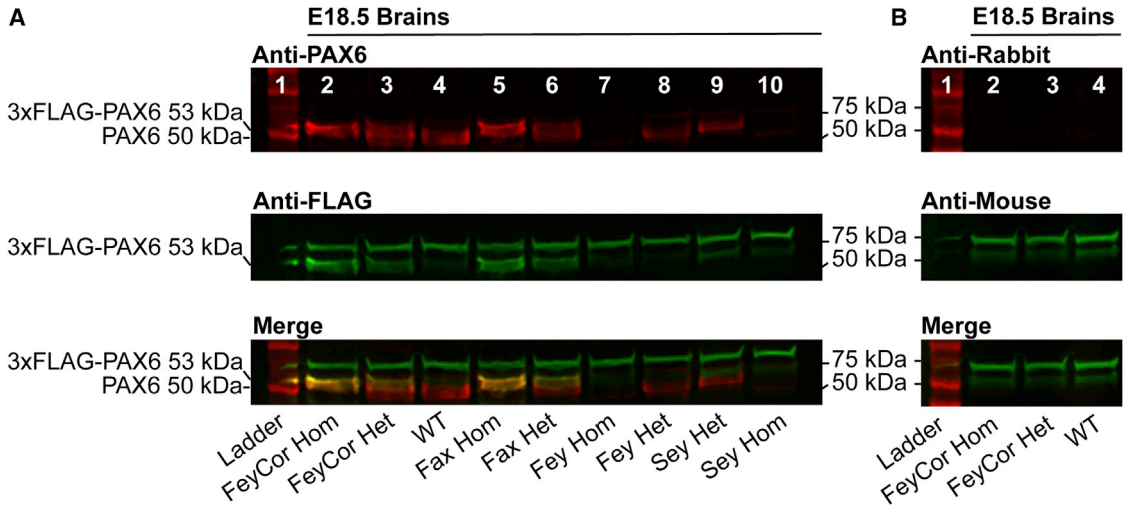

Figure 7. Expression of 3xFLAG-PAX6 Was Confirmed in *Fax* and *FeyCor* Mice

Total protein was collected from mouse brains for western blot analysis with PAX6 (red) and FLAG (green) antibodies at embryonic day 18.5 (E18.5). (A) Anti-PAX6 detected a doublet of both 3xFLAG-PAX6 (53-kDa) and PAX6 (50-kDa) proteins in lanes 3 and 6. Anti-FLAG identified the 3xFLAG-PAX6 protein. Merge showed positive co-staining with both antibodies. (B) Secondary antibody control. In the absence of the primary antibodies, the anti-mouse secondary antibody detected non-specific mouse proteins at ~75 and ~55 kDa; the former stronger band was used as the loading control. *FeyCor*, *Fey* corrected; *Fax*, FLAG-tagged *Pax6*; *Fey*, FLAG-tagged *Sey*.

will need empirical testing. PAX6 plays a critical role in maintaining the corneal limbal stem cell (LSC) niche in both human and mouse eyes. LSC deficiency is the underlying mechanism responsible for cornea opacification and ultimately blindness in aniridia.[57–60] Hence, in future studies, we aim to deliver our CRISPR strategy to LSCs of post-weaned *Fey* mice to model gene therapy in recently diagnosed children with aniridia.

Taken together, we have created a novel mouse model for testing CRISPR-based genome editing, as well as other therapeutic approaches for preclinical assay development for aniridia. We demonstrated that germline correction of the *Sey* mutation alone rescues the mutant phenotype. Finally, we have developed an allele-distinguishing CRISPR strategy that corrected the *Sey* mutation in both cells and the mouse germline.

MATERIALS AND METHODS

Cloning

To generate plasmids for *in vitro* transcription, EmGFP, *PAX6*, 3xFLAG/*PAX6*, and *PAX6*/3xFLAG open reading frames (ORFs) were cloned into pBluescript as previously described.[12,61] Briefly, EmGFP, *PAX6*, 3xFLAG/*PAX6*, and *PAX6*/3xFLAG ORFs, flanked by *Not*I restriction sites, were commercially synthesized (DNA2.0, Menlo Park, CA, USA). pBluescript and DNA2.0 plasmids containing EmGFP, *PAX6*, 3xFLAG/*PAX6*, and *PAX6*/3xFLAG were electroporated into 50 μL of OneShot TOP 10 Electrocomp *Escherichia coli* (C404052; Thermo Fisher Scientific, Waltham, MA, USA) as directed, and cultured on Luria-Bertani (LB) plates. Resulting colonies were picked and cultured, and the DNA was prepped (27104; QIAGEN, Germantown, MD, USA). The resulting plasmids were digested with *Not*I (R0189; New England Biolabs, Ipswich, MA, USA), size separated, and gel extracted, and the ORFs were ligated into pBluescript using T4 DNA ligase (M0202; New England Biolabs). Ligation products were electroporated into TOP 10 cells, cultured, and DNA was prepared as described above. Correct ligation was confirmed by restriction digest with *Nco*I (R0193; New England Biolabs) and *Xho*I (R0146; New England Biolabs), as well as Sanger sequencing that was executed at the Centre for Molecular Medicine and Therapeutics (CMMT) DNA Sequencing Core Facility.

mRNA Production and Injection into *X. laevis*

To produce mRNA for injection into *X. laevis* embryos, EmGFP, *PAX6*, 3xFLAG/*PAX6*, and *PAX6*/3xFLAG ORFs were *in vitro* transcribed, polyadenylated, and 5′ capped. Plasmids were linearized and the T7 promoter was used to produce 5′ capped, polyadenylated mRNA using the mMESSAGE mMACHINE T7 ultra kit (AM1345; Thermo Fisher Scientific) as directed. The integrity of the resulting mRNA was confirmed by gel electrophoresis, and mRNA concentration was determined using a NanoDrop spectrophotometer. *X. laevis* females were injected with 700 U of human chorionic gonadotropin and housed in 18°C tadpole Ringer's solution overnight. Embryos were produced by *in vitro* fertilization, and 50 ng of mRNA was injected into each embryo at the 16-cell stage. The resulting embryos were reared in 18°C tadpole Ringer's solution, in 4-L tanks, on a 12-h light/12-h dark cycle. Fourteen days after conception, tadpoles were fixed in 4% paraformaldehyde (PFA) and screened for the formation of ectopic eye structures using a white light dissecting microscope.

Cell Culture

Pax6$^{Sey/Sey}$ and *Pax6*$^{+/+}$ ESCs were produced by setting up timed pregnancies with B6-*Pax6*$^{Sey/+}$ dam mice and 129-*Pax6*$^{Sey/+}$ stud

males and B6-*Pax6*$^{+/+}$ dam mice and 129-*Pax6*$^{+/+}$ stud males, respectively. The resulting embryos were harvested and treated as previously described.[62] The ESCs were cultured in high-glucose Dulbecco's modified Eagle's medium (DMEM) (LS11960044; Thermo Fisher Scientific) supplemented with 1,000 U/mL ESGRO recombinant mouse leukemia inhibitory factor (ESG1107; Chemicon/MilliporeSigma, Burlington, MA, USA), 16% fetal bovine serum (080-150; Wisent Bioproducts, Canada), 0.1 mM MEM non-essential amino acids solution (11140050; Thermo Fisher Scientific), 2 mM L-glutamine (25030081; Thermo Fisher Scientific), and 0.01% 2-mercaptoethanol (M7522; Sigma-Aldrich, St. Louis, MO). ESC lines were genotyped for *Pax6* using a WT-specific polymerase chain reaction (PCR) assay with primer pair oEMS6076 (5′-AACACCAACTCCATCAGTTCTAATG-3′) and oEMS6075 (5′-GCAAAATATAAGCATCCCAGTGCAT-3′), as well as a *Sey*-specific PCR assay with primer pair oEMS6071 (5′-TC ACTCTATTTTCCCAACACAGCC-3′) and oEMS6073 (5′-CTG AGCTTCATCCGAGTCTTCTTA-3′). The selected ESC lines were expanded on mouse embryonic fibroblast cells until passage 8. Subsequently, the cells were maintained on tissue culture plates coated with 0.1% gelatin (G7-500; Thermo Fisher Scientific) in sterile distilled water for a minimum of five passages prior to use in *in vitro* gene editing experiments.

In Vitro Gene Editing

The online tool Benchling (https://benchling.com/crispr) was used to design gRNAs for the *Streptococcus pyogenes* Cas9 nuclease in the region of interest. The top three gRNAs were selected based on their predicted on-target and off-target effects, and their proximity to either the *Pax6* start codon for 3xFLAG insertion, or the *Sey* mutation for the correction strategy. The commercially synthesized CRISPR RNA (crRNA) and *trans*-activating crRNA (tracrRNA) (GenScript, Piscataway, NJ, USA) were annealed at a 1:1 ratio by incubating at 95°C for 5 min to generate gRNA. Next, ssODN templates with 60- to 80-bp homology on each side of a Cas9 cleavage site were ordered (Integrated DNA Technologies, Coralville, IA, USA). When required, a silent mutation was introduced in PAM to prevent Cas9 nuclease from re-cleaving the desired sequence after the initial editing step. A purified highly concentrated Cas9 nuclease protein with nuclear localization signal (CP02; PNA Bio, Thousand Oaks, CA, USA), which is suitable for electroporation, was purchased. The Cas9 and gRNA stocks were 5 and 3.3 μg/μL, respectively. For 3xFLAG insertion, the ssODN concentration was 12 μg/μL, while the ssODN concentration for the *Sey* correction was 10 μg/μL. A 10-μL Neon transfection system tip was used according to the manufacturer's protocol (Thermo Fisher Scientific) to deliver the CRISPR components into ESCs. Briefly, the RNP complex was formed by mixing 0.3 μL of Cas9 with 0.2 μL of annealed gRNA and incubated at room temperature for 20 min. Right before electroporation, 0.3 μL of ssODN was added to the RNP complex. 2×10^5 cells were used for each reaction with Neon optimization setting 14, which was previously determined to best suit our cells. Electroporated cells were plated as duplicates in a 24-well plate containing pre-warmed media. The plate was incubated in a 37°C incubator with 5% CO_2. At 48 h post-electroporation, cells were lysed in tissue homogenization buffer (THB) according to a previously described protocol.[62] The sequences for the best performed crRNAs and ssODNs are listed in Table S1.

Sanger and Site-Specific NGS

The region around *Sey* mutation was PCR amplified using a Q5 high-fidelity PCR kit (E0555S; New England Biolabs), with primer pair oEMS6299 (5′-ATGCCGTTCCGATTTCTC-3′) and oEMS6171 (5′-GCTGTGGCATTTCCTTTG-3′). Following gel electrophoresis, DNA bands were excised and purified using a QIAquick gel purification kit (29706; QIAGEN). Cleaned DNA samples were then sent to the CMMT DNA Sequencing Core Facility for Sanger sequencing using the same primers as above.

Whole-cell lysates from electroporated cells were sent to Desktop Genetics (London, UK) to be assayed for gene-editing frequency by site-specific NGS with self-designed primers.

Mouse Husbandry

All mice were bred and maintained in the pathogen-free mouse core facility of the CMMT at the University of British Columbia (UBC). Animal work was performed in accordance with the guidelines set by the Canadian Council on Animal Care and adhered to the Association for Research in Vision and Ophthalmology statement for the use of animals in ophthalmic and vision research. All work was done following protocols approved by the UBC Animal Care Committee (protocols A17-0204 and A17-0205). For characterizing the strains, WT B6 (The Jackson Laboratory [JAX] strain code 000664) dams were bred with heterozygous transgenic sires (backcross N2 or higher). Pups were weaned and ear notched at postnatal day 21. Collected ear notches were digested in THB with protein kinase and genotyped by PCR using primer pair oEMS6145 (5′-GATTCTC CAGTTCAGGCACC-3′) and oEMS6146 (5′-CTCAGTGTTGC CCGGATAGA-3′) and primer pair oEMS6077 (5′-CGTATATCC CAGTTCTCAGGC-3′) and oEMS6144 (5′-CTTGTCATCGT CATCCTTGT-3′), allowing for detection of 3xFLAG insertion based on size difference and sequence specificity, respectively. Primer pairs used for WT and *Sey*-specific PCR assays were as mentioned earlier. For phenotyping the *Fax* strain, WT and homozygous *Fax* mice littermates (N2F2 or higher) obtained from intercrosses were used to set up WT or *Fax* incrosses. The progeny eyes were scored for abnormal phenotypes by visual inspection at 4 weeks, and representative eyes were imaged by slit lamp at a minimum of 3 months of age.

In Vivo Gene Editing

For the creation of the *Fey* and *Fax* strains, zygotes from day 0.5 post-coitus (PC) plugs were obtained by the superovulation of B6 females mated with B6-*Pax6*$^{Sey/+}$ and B6 males, respectively. For the *FeyCor* strain, superovulated *Pax6*$^{Fey/+}$ females were set up with B6 males. The day of injection, all females were plug checked, and only those with a PC plug present were harvested. Zygotes were harvested into a EmbryoMax M2 medium (MR-015-D; MilliporeSigma) or Research Vitro Wash (K-RVWA-50; Cook Medical, Bloomington, IN, USA), then treated with a 300 μg/mL solution of hyaluronidase (H272; Sigma-Aldrich) to remove cumulus cells. Zygotes were then placed

into cultured KSOM (potassium simplex optimization medium) (MR-121-D; MilliporeSigma) or Research Vitro Cleave (K-RVCL-50; Cook Medical) medium until the time of injection. The CRISPR RNP complex was formed immediately prior to microinjection by mixing 2.5 μL of 1 μg/μL Cas9 (CP01-20; PNA Bio) with 3.8 μL of 0.3 μg/μL crRNA/tracrRNA (GenScript) and incubating the mixture on ice for 10 min. For 3xFLAG insertion, 4.3 μL of 1.2 μg/μL ssODN (Integrated DNA Technologies) was added to the corresponding complexed RNP and the mixture was topped up to 50 μL using an embryo-grade Tris-EDTA (TE) buffer (CytoSpring, Mountain View, CA, USA). For the *Sey* germline correction, 5.1 μL of 1 μg/μL ssODN (Integrated DNA Technologies) was used in the final 50-μL reaction. The injection mix was filtered using a 0.45-μm Millex filter (SLHVR04NL; MilliporeSigma), and injections were done into the cytoplasm of one-cell mouse zygotes using the XenoWorks digital microinjection system (Sutter Instrument, Novato, CA, USA). Post-microinjection zygotes were placed back into KSOM and incubated until transferred into day 0.5 PC pseudopregnant CD-1 females (Charles River strain code 022). The sequences of crRNAs and ssODNs used in the microinjection are listed in Table S1.

Slit Lamp Imaging

Adult mice (2–4 months old) were placed in the induction chamber and induced with isoflurane using a SomnoSuite (Kent Scientific, Torrington, CA, USA). After the induction phase, the mice were transferred to the nose cone and eyes were covered with 1% Isopto Tears ophthalmic solution (Alcon, Geneva, Switzerland). A Micron IV retinal imaging microscope (Phoenix Research Labs, Pleasanton, CA, USA) with an anterior segment slit lamp attachment was used to image the eyes.

Immunohistological Analysis and Image Processing

After slit lamp imaging, mice were sacrificed by cervical dislocation while still under anesthesia. Eyes were immediately enucleated and directly fixed in 4% PFA (P6148; Sigma-Aldrich) in Dulbecco's phosphate-buffered saline (DPBS) (14190-144; Thermo Fisher Scientific) for 2 h on ice. Subsequently, eyes were immersed in 25% sucrose (S8501; Sigma-Aldrich) in DPBS solution with 0.02% sodium azide (S8032; Sigma-Aldrich) at 4°C overnight. The next day, eyes were orientated in a mold containing Tissue-Tek OCT compound (4583; Sakura Finetek, Torrance, CA, USA) and incubated for 1 h at room temperature before being frozen using dry ice. The blocks were sectioned at 20 μm with a Microm HM550 cryostat (Thermo Scientific, Waltham, MA, USA). For immunofluorescence staining, sections were processed and mounted as previously described,[63] with the difference that antigen retrieval was performed by incubating the slides in freshly made citrate buffer (10 mM sodium citrate, 0.05% Tween 20 [pH 6.0]) for 1 h at 55°C, prior to the blocking step that lasted for 1 h at room temperature. Primary antibodies used were rabbit anti-PAX6 (1:1,000; 901301; BioLegend, San Diego, CA, USA) and mouse anti-FLAG (1:500; F3165; Sigma-Aldrich). Secondary antibodies used were anti-rabbit immunoglobulin G (IgG) (1:1,000; A11037; Thermo Fisher Scientific) and anti-mouse IgG (1:1,000; A11029; Thermo Fisher Scientific). Eleven z-stack images were taken at 0.5 μm intervals on a Leica SP8 confocal microscope (Leica Microsystems, Wetzlar, DE, USA) at ×40 magnification. Conservative deconvolution of the raw data was carried out using Huygens Professional software (Scientific Volume Imaging, Hilversum, the Netherlands). The resulting images were stacked at sum slices projection using ImageJ software (https://imagej.nih.gov/ij/, version 1.48). The final images were flattened and exported as tagged image file format (TIFF) files.

E18.5 Fetus Generation

A previously described, timed pregnancy protocol was followed.[61] Heterozygous dams and sires were bred, producing homozygous, heterozygous, and WT offspring for each strain. On E18.5, pregnant dams were sacrificed by cervical dislocation and their uteruses were removed. Fetuses were isolated by removing the yolk sac. Fetuses were imaged at ×0.8 magnification using a Leica MZ125 microscope with a CoolSnap-Pro CF camera (Leica Microsystems). Fetuses were then decapitated and brains were collected. Brains were divided into hemispheres by directly cutting down the longitudinal fissure. Each hemisphere was flash-frozen in liquid nitrogen and stored at −80°C. Lastly, tail tip samples were taken to be used in PCR-based genotyping of the E18.5 fetuses.

Western Blot Analysis

Protein extraction, quantification, and western blotting were performed according to a previously described protocol.[39] Briefly, E18.5 brain hemispheres were homogenized in lysis buffer. The extracted proteins were quantified and 34 μg of each protein sample was run on the gel before being transferred to the polyvinylidene fluoride (PVDF) membrane. The blots were blocked and incubated with primary antibodies against PAX6 (1:1,000; 901301, BioLegend) and FLAG (1:500; F3165, Sigma-Aldrich). Blots were washed and incubated with anti-rabbit (1:5,000; A11037; Thermo Fisher Scientific) and anti-mouse (1:10,000; A11029; Thermo Fisher Scientific) secondary antibodies. After the final wash, the fluorescence signals were detected using the LI-COR Odyssey imaging system (LI-COR Biosciences, Lincoln, NE, USA).

SUPPLEMENTAL INFORMATION

Supplemental Information can be found online at https://doi.org/10.1016/j.omtm.2020.03.002.

AUTHOR CONTRIBUTIONS

Conceptualization, E.M.S.; Methodology, S.Z.M.M., J.W.H., and S.L.L.; Investigation, S.Z.M.M., J.W.H., S.L.L., N.Y.C., T.C.L., and B.M.T.; Writing – Original Draft, S.Z.M.M.; Writing – Review & Editing, E.M.S.; Visualization, S.Z.M.M., J.W.H., and B.M.T.; Supervision, O.L.M. and E.M.S.; Funding Acquisition, O.L.M. and E.M.S.

CONFLICTS OF INTEREST

The authors declare no competing interests.

ACKNOWLEDGMENTS

We thank Tom W. Johnson, of the Mouse Animal Production Service (MAPS), for making the *Fey* mouse. We also thank Dr. Jingsong Wang at the British Columbia Children's Hospital Research (BCCHR) Institute Imaging Core Facility for access to the confocal microscope and Dr. Elizabeth Hui at the BCCHR Institute Sequencing and Bioanalyzer Core for Sanger sequencing support. This work was funded by a Canadian Institutes of Health Research (CIHR) grant (2OR77895) awarded to E.M.S. The Micron IV retinal imaging microscope and SomnoSuite were funded by the Canada Foundation for Innovation (CFI) (grant 2OR76139) and the BCCHR Institute (grant CRG74760), respectively. Additionally, salary support was provided to S.Z.M.M. by the Brain Canada Foundation through the Canada Brain Research Fund, with the financial support of Health Canada and the BCCHR Institute. The views expressed herein do not necessarily represent the views of the Minister of Health or the Government of Canada. We also acknowledge salary support to J.W.H. from the University of British Columbia Four Year Doctoral Fellowship and Graduate Student Initiatives, and the CIHR Canadian Graduate Scholarship.

REFERENCES

1. Simpson, T.I., and Price, D.J. (2002). Pax6; a pleiotropic player in development. BioEssays *24*, 1041–1051.
2. Tyas, D.A., Simpson, T.I., Carr, C.B., Kleinjan, D.A., van Heyningen, V., Mason, J.O., and Price, D.J. (2006). Functional conservation of *Pax6* regulatory elements in humans and mice demonstrated with a novel transgenic reporter mouse. BMC Dev. Biol. *6*, 21.
3. Vincent, M.C., Pujo, A.L., Olivier, D., and Calvas, P. (2003). Screening for *PAX6* gene mutations is consistent with haploinsufficiency as the main mechanism leading to various ocular defects. Eur. J. Hum. Genet. *11*, 163–169.
4. Calvão-Pires, P., Santos-Silva, R., Falcão-Reis, F., and Rocha-Sousa, A. (2014). Congenital aniridia: clinic, genetics, therapeutics, and prognosis. Int. Sch. Res. Notices *2014*, 305350.
5. Tsai, J.H., Freeman, J.M., Chan, C.C., Schwartz, G.S., Derby, E.A., Petersen, M.R., and Holland, E.J. (2005). A progressive anterior fibrosis syndrome in patients with post-surgical congenital aniridia. Am. J. Ophthalmol. *140*, 1075–1079.
6. Edén, U., Riise, R., and Tornqvist, K. (2010). Corneal involvement in congenital aniridia. Cornea *29*, 1096–1102.
7. Naldini, L. (2015). Gene therapy returns to centre stage. Nature *526*, 351–360.
8. Schedl, A., Ross, A., Lee, M., Engelkamp, D., Rashbass, P., van Heyningen, V., and Hastie, N.D. (1996). Influence of *PAX6* gene dosage on development: overexpression causes severe eye abnormalities. Cell *86*, 71–82.
9. Ouyang, J., Shen, Y.C., Yeh, L.K., Li, W., Coyle, B.M., Liu, C.Y., and Fini, M.E. (2006). *Pax6* overexpression suppresses cell proliferation and retards the cell cycle in corneal epithelial cells. Invest. Ophthalmol. Vis. Sci. *47*, 2397–2407.
10. Manuel, M., Pratt, T., Liu, M., Jeffery, G., and Price, D.J. (2008). Overexpression of Pax6 results in microphthalmia, retinal dysplasia and defective retinal ganglion cell axon guidance. BMC Dev. Biol. *8*, 59.
11. Davis, J., and Piatigorsky, J. (2011). Overexpression of Pax6 in mouse cornea directly alters corneal epithelial cells: changes in immune function, vascularization, and differentiation. Invest. Ophthalmol. Vis. Sci. *52*, 4158–4168.
12. Hickmott, J.W., Chen, C.Y., Arenillas, D.J., Korecki, A.J., Lam, S.L., Molday, L.L., Bonaguro, R.J., Zhou, M., Chou, A.Y., Mathelier, A., et al. (2016). *PAX6* MiniPromoters drive restricted expression from rAAV in the adult mouse retina. Mol. Ther. Methods Clin. Dev. *3*, 16051.
13. Ran, F.A., Hsu, P.D., Wright, J., Agarwala, V., Scott, D.A., and Zhang, F. (2013). Genome engineering using the CRISPR-Cas9 system. Nat. Protoc. *8*, 2281–2308.
14. Kosicki, M., Tomberg, K., and Bradley, A. (2018). Repair of double-strand breaks induced by CRISPR-Cas9 leads to large deletions and complex rearrangements. Nat. Biotechnol. *36*, 765–771.
15. Gehring, W.J. (1996). The master control gene for morphogenesis and evolution of the eye. Genes Cells *1*, 11–15.
16. Roberts, R.C. (1967). Small-eyes, a new dominant mutant in the mouse. Genet. Res. *9*, 121–122.
17. Hogan, B.L., Horsburgh, G., Cohen, J., Hetherington, C.M., Fisher, G., and Lyon, M.F. (1986). *Small eyes* (*Sey*): a homozygous lethal mutation on chromosome 2 which affects the differentiation of both lens and nasal placodes in the mouse. J. Embryol. Exp. Morphol. *97*, 95–110.
18. Hill, R.E., Favor, J., Hogan, B.L., Ton, C.C., Saunders, G.F., Hanson, I.M., Prosser, J., Jordan, T., Hastie, N.D., and van Heyningen, V. (1991). Mouse small eye results from mutations in a paired-like homeobox-containing gene. Nature *354*, 522–525.
19. Ramaesh, T., Collinson, J.M., Ramaesh, K., Kaufman, M.H., West, J.D., and Dhillon, B. (2003). Corneal abnormalities in $Pax6^{+/-}$ small eye mice mimic human aniridia-related keratopathy. Invest. Ophthalmol. Vis. Sci. *44*, 1871–1878.
20. Yokoi, T., Nishina, S., Fukami, M., Ogata, T., Hosono, K., Hotta, Y., and Azuma, N. (2016). Genotype-phenotype correlation of *PAX6* gene mutations in aniridia. Hum. Genome Var. *3*, 15052.
21. Hever, A.M., Williamson, K.A., and van Heyningen, V. (2006). Developmental malformations of the eye: the role of *PAX6*, *SOX2* and *OTX2*. Clin. Genet. *69*, 459–470.
22. Sansom, S.N., Griffiths, D.S., Faedo, A., Kleinjan, D.J., Ruan, Y., Smith, J., van Heyningen, V., Rubenstein, J.L., and Livesey, F.J. (2009). The level of the transcription factor Pax6 is essential for controlling the balance between neural stem cell self-renewal and neurogenesis. PLoS Genet. *5*, e1000511.
23. Gregory-Evans, C.Y., Wang, X., Wasan, K.M., Zhao, J., Metcalfe, A.L., and Gregory-Evans, K. (2014). Postnatal manipulation of *Pax6* dosage reverses congenital tissue malformation defects. J. Clin. Invest. *124*, 111–116.
24. Wang, X., Gregory-Evans, K., Wasan, K.M., Sivak, O., Shan, X., and Gregory-Evans, C.Y. (2017). Efficacy of postnatal in vivo nonsense suppression therapy in a *Pax6* mouse model of aniridia. Mol. Ther. Nucleic Acids *7*, 417–428.
25. Hung, S.S., Chrysostomou, V., Li, F., Lim, J.K., Wang, J.H., Powell, J.E., Tu, L., Daniszewski, M., Lo, C., Wong, R.C., et al. (2016). AAV-mediated CRISPR/Cas gene editing of retinal cells in vivo. Invest. Ophthalmol. Vis. Sci. *57*, 3470–3476.
26. Ruan, G.X., Barry, E., Yu, D., Lukason, M., Cheng, S.H., and Scaria, A. (2017). CRISPR/Cas9-mediated genome editing as a therapeutic approach for Leber congenital amaurosis 10. Mol. Ther. *25*, 331–341.
27. Yu, W., Mookherjee, S., Chaitankar, V., Hiriyanna, S., Kim, J.W., Brooks, M., Ataeijannati, Y., Sun, X., Dong, L., Li, T., et al. (2017). *Nrl* knockdown by AAV-delivered CRISPR/Cas9 prevents retinal degeneration in mice. Nat. Commun. *8*, 14716.
28. McCullough, K.T., Boye, S.L., Fajardo, D., Calabro, K., Peterson, J.J., Strang, C.E., Chakraborty, D., Gloskowski, S., Haskett, S., and Samuelsson, S. (2019). Somatic gene editing of GUCY2D by AAV-CRISPR/Cas9 alters retinal structure and function in mouse and macaque. Hum. Gene Ther *30*, 571–589.
29. Giannelli, S.G., Luoni, M., Castoldi, V., Massimino, L., Cabassi, T., Angeloni, D., Demontis, G.C., Leocani, L., Andreazzoli, M., and Broccoli, V. (2018). Cas9/sgRNA selective targeting of the P23H *Rhodopsin* mutant allele for treating retinitis pigmentosa by intravitreal AAV9.PHP.B-based delivery. Hum. Mol. Genet. *27*, 761–779.
30. Jo, D.H., Song, D.W., Cho, C.S., Kim, U.G., Lee, K.J., Lee, K., Park, S.W., Kim, D., Kim, J.H., and Kim, J.S. (2019). CRISPR-Cas9-mediated therapeutic editing of Rpe65 ameliorates the disease phenotypes in a mouse model of Leber congenital amaurosis. Sci. Adv *5*, eaax1210.
31. Hopp, T., Prickett, K., Price, V., Libby, R., March, C., Cerretti, D., Urdal, D.L., and Conlon, P.J. (1988). A short polypeptide marker sequence useful for recombinant protein identification and purification. Nat. Biotechnol. *6*, 1204–1210.
32. Terpe, K. (2003). Overview of tag protein fusions: from molecular and biochemical fundamentals to commercial systems. Appl. Microbiol. Biotechnol. *60*, 523–533.
33. Chow, R.L., Altmann, C.R., Lang, R.A., and Hemmati-Brivanlou, A. (1999). Pax6 induces ectopic eyes in a vertebrate. Development *126*, 4213–4222.

34. Karmakar, U.K., Ishikawa, N., Toume, K., Arai, M.A., Sadhu, S.K., Ahmed, F., and Ishibashi, M. (2015). Sesquiterpenes with TRAIL-resistance overcoming activity from *Xanthium strumarium*. Bioorg. Med. Chem. *23*, 4746–4754.

35. Wawersik, S., and Maas, R.L. (2000). Vertebrate eye development as modeled in *Drosophila*. Hum. Mol. Genet. *9*, 917–925.

36. Aota, S., Nakajima, N., Sakamoto, R., Watanabe, S., Ibaraki, N., and Okazaki, K. (2003). *Pax6* autoregulation mediated by direct interaction of Pax6 protein with the head surface ectoderm-specific enhancer of the mouse *Pax6* gene. Dev. Biol. *257*, 1–13.

37. Gan, Q., Lee, A., Suzuki, R., Yamagami, T., Stokes, A., Nguyen, B.C., Pleasure, D., Wang, J., Chen, H.W., and Zhou, C.J. (2014). *Pax6* mediates β-catenin signaling for self-renewal and neurogenesis by neocortical radial glial stem cells. Stem Cells *32*, 45–58.

38. Jang, E.S., and Goldman, J.E. (2011). *Pax6* expression is sufficient to induce a neurogenic fate in glial progenitors of the neonatal subventricular zone. PLoS ONE *6*, e20894.

39. Hickmott, J.W., Gunawardane, U., Jensen, K., Korecki, A.J., and Simpson, E.M. (2018). Epistasis between *Pax6*^{Sey} and genetic background reinforces the value of defined hybrid mouse models for therapeutic trials. Gene Ther. *25*, 524–537.

40. Monteys, A.M., Ebanks, S.A., Keiser, M.S., and Davidson, B.L. (2017). CRISPR/Cas9 editing of the mutant huntingtin allele in vitro and in vivo. Mol. Ther. *25*, 12–23.

41. Li, P., Kleinstiver, B.P., Leon, M.Y., Prew, M.S., Navarro-Gomez, D., Greenwald, S.H., Pierce, E.A., Joung, J.K., and Liu, Q. (2018). Allele-specific CRISPR-Cas9 genome editing of the single-base P23H mutation for rhodopsin-associated dominant retinitis pigmentosa. CRISPR J. *1*, 55–64.

42. Christie, K.A., Courtney, D.G., DeDionisio, L.A., Shern, C.C., De Majumdar, S., Mairs, L.C., Nesbit, M.A., and Moore, C.B.T. (2017). Towards personalised allele-specific CRISPR gene editing to treat autosomal dominant disorders. Sci. Rep. *7*, 16174.

43. Hough, S.H., Ajetunmobi, A., Brody, L., Humphryes-Kirilov, N., and Perello, E. (2016). Desktop genetics. Per. Med. *13*, 517–521.

44. Pfeiffer, F., Gröber, C., Blank, M., Händler, K., Beyer, M., Schultze, J.L., and Mayer, G. (2018). Systematic evaluation of error rates and causes in short samples in next-generation sequencing. Sci. Rep. *8*, 10950.

45. Glaser, T., Jepeal, L., Edwards, J.G., Young, S.R., Favor, J., and Maas, R.L. (1994). PAX6 gene dosage effect in a family with congenital cataracts, aniridia, anophthalmia and central nervous system defects. Nat. Genet. *7*, 463–471.

46. Samant, M., Chauhan, B.K., Lathrop, K.L., and Nischal, K.K. (2016). Congenital aniridia: etiology, manifestations and management. Expert Rev. Ophthalmol. *11*, 135–144.

47. Fahey, J.R., Katoh, H., Malcolm, R., and Perez, A.V. (2013). The case for genetic monitoring of mice and rats used in biomedical research. Mamm. Genome *24*, 89–94.

48. Barton-Davis, E.R., Cordier, L., Shoturma, D.I., Leland, S.E., and Sweeney, H.L. (1999). Aminoglycoside antibiotics restore dystrophin function to skeletal muscles of mdx mice. J. Clin. Invest. *104*, 375–381.

49. Heier, C.R., and DiDonato, C.J. (2009). Translational readthrough by the aminoglycoside geneticin (G418) modulates SMN stability in vitro and improves motor function in SMA mice in vivo. Hum. Mol. Genet. *18*, 1310–1322.

50. Brasell, E.J., Chu, L., El Kares, R., Seo, J.H., Loesch, R., Iglesias, D.M., and Goodyer, P. (2019). The aminoglycoside geneticin permits translational readthrough of the *CTNS* W138X nonsense mutation in fibroblasts from patients with nephropathic cystinosis. Pediatr. Nephrol. *34*, 873–881.

51. Gonzalez-Hilarion, S., Beghyn, T., Jia, J., Debreuck, N., Berte, G., Mamchaoui, K., Mouly, V., Gruenert, D.C., Déprez, B., and Lejeune, F. (2012). Rescue of nonsense mutations by amlexanox in human cells. Orphanet J. Rare Dis. *7*, 58.

52. Atanasova, V.S., Jiang, Q., Prisco, M., Gruber, C., Piñón Hofbauer, J., Chen, M., Has, C., Bruckner-Tuderman, L., McGrath, J.A., Uitto, J., and South, A.P. (2017). Amlexanox enhances premature termination codon read-through in *COL7A1* and expression of full length type VII collagen: potential therapy for recessive dystrophic epidermolysis bullosa. J. Invest. Dermatol. *137*, 1842–1849.

53. Sahel, J.A., and Marazova, K. (2014). Toward postnatal reversal of ocular congenital malformations. J. Clin. Invest. *124*, 81–84.

54. Cox, D.B.T., Gootenberg, J.S., Abudayyeh, O.O., Franklin, B., Kellner, M.J., Joung, J., and Zhang, F. (2017). RNA editing with CRISPR-Cas13. Science *358*, 1019–1027.

55. Ohmori, T., Nagao, Y., Mizukami, H., Sakata, A., Muramatsu, S.I., Ozawa, K., Tominaga, S.I., Hanazono, Y., Nishimura, S., Nureki, O., and Sakata, Y. (2017). CRISPR/Cas9-mediated genome editing via postnatal administration of AAV vector cures haemophilia B mice. Sci. Rep. *7*, 4159.

56. Berger, A., Lorain, S., Joséphine, C., Desrosiers, M., Peccate, C., Voit, T., Garcia, L., Sahel, J.A., and Bemelmans, A.P. (2015). Repair of rhodopsin mRNA by spliceosome-mediated RNA trans-splicing: a new approach for autosomal dominant retinitis pigmentosa. Mol. Ther. *23*, 918–930.

57. Ramaesh, K., Ramaesh, T., Dutton, G.N., and Dhillon, B. (2005). Evolving concepts on the pathogenic mechanisms of aniridia related keratopathy. Int. J. Biochem. Cell Biol. *37*, 547–557.

58. Mort, R.L., Bentley, A.J., Martin, F.L., Collinson, J.M., Douvaras, P., Hill, R.E., Morley, S.D., Fullwood, N.J., and West, J.D. (2011). Effects of aberrant *Pax6* gene dosage on mouse corneal pathophysiology and corneal epithelial homeostasis. PLoS ONE *6*, e28895.

59. Li, G., Xu, F., Zhu, J., Krawczyk, M., Zhang, Y., Yuan, J., Patel, S., Wang, Y., Lin, Y., Zhang, M., et al. (2015). Transcription factor PAX6 (paired box 6) controls limbal stem cell lineage in development and disease. J. Biol. Chem. *290*, 20448–20454.

60. Roux, L.N., Petit, I., Domart, R., Concordet, J.P., Qu, J., Zhou, H., Joliot, A., Ferrigno, O., and Aberdam, D. (2018). Modeling of aniridia-related keratopathy by CRISPR/Cas9 genome editing of human limbal epithelial cells and rescue by recombinant PAX6 protein. Stem Cells *36*, 1421–1429.

61. de Leeuw, C.N., Korecki, A.J., Berry, G.E., Hickmott, J.W., Lam, S.L., Lengyell, T.C., Bonaguro, R.J., Borretta, L.J., Chopra, V., Chou, A.Y., et al. (2016). rAAV-compatible MiniPromoters for restricted expression in the brain and eye. Mol. Brain *9*, 52.

62. Yang, G.S., Banks, K.G., Bonaguro, R.J., Wilson, G., Dreolini, L., de Leeuw, C.N., Liu, L., Swanson, D.J., Goldowitz, D., Holt, R.A., and Simpson, E.M. (2009). Next generation tools for high-throughput promoter and expression analysis employing single-copy knock-ins at the *Hprt1* locus. Genomics *93*, 196–204.

63. Korecki, A.J., Hickmott, J.W., Lam, S.L., Dreolini, L., Mathelier, A., Baker, O., Kuehne, C., Bonaguro, R.J., Smith, J., Tan, C.V., et al. (2019). Twenty-seven tamoxifen-inducible iCre-driver mouse strains for eye and brain, including seventeen carrying a new inducible-first constitutive-ready allele. Genetics *211*, 1155–1177.